Coulomb excitation effects in neutron transfer reactions

Helvetica Physica Acta
Vol. 45, 1972.

Birkhäuser Verlag Basel

Coulomb Excitation Effects in Neutron Transfer Reactions

by **R. H. Morf** and **K. Alder**
Institute of Theoretical Physics, University of Basle, Basle

(3. VIII. 72)

Abstract. A time-dependent semiclassical picture is used to describe the virtual Coulomb excitation occurring in subcoulomb neutron transfer reactions. This leads to coupled differential equations for the amplitudes of the nuclear states involved. Numerical results of the virtual electric quadrupole excitation effects are given for typical neutron transfer reactions.

1. Introduction

During the last couple of years, neutron transfer reactions have been extensively employed for the investigation of nuclear structure. In order to avoid uncertainties in the description of the forces which determine the scattering process, it has been suggested to study the neutron transfer reactions (NTR) in the subcoulomb energy range. Although this brings in small transfer cross-sections, eventually leading to high experimental statistical error, the less model dependent description which is then possible more than outweighs this disadvantage.

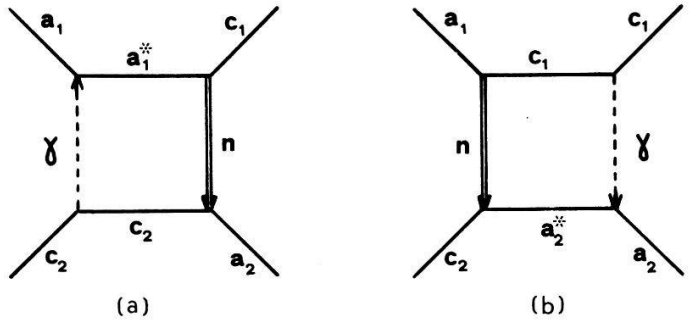

Figure 1
Diagram (a) shows the Coulomb excitation of the projectile before the neutron is exchanged. Diagram (b) shows the excitation of the target after the neutron transfer. Excited states are marked by an asterisk.

A DWBA theory of NTR has been developed by Buttle and Goldfarb [1]. They have not only given an expression for the pure transfer transition, but, within the framework of the DWBA, they have also theoretically taken into account target Coulomb excitation effects. It has long been advocated [2] that neglecting the possibility of virtual Coulomb excitation in NTR could lead to a misinterpretation of the experimental results. In an intuitive way, it is easy to imagine that, especially under experimental conditions where the neutron transfer from the projectile ground state is unfavourable, the effects of projectile excitation (Fig. 1a) may lead to a considerable

change of the transfer cross-sections. Similarly, final target states which are little populated by the direct neutron transfer transition, may receive an appreciable contribution to their amplitudes through the indirect transitions via a neighbour level (Fig. 1b). This shows that the neutron transfer cross-sections will depend upon the electric multipole moments of the nuclear states involved. It gives us some hope that from accurate measurements of differential transfer cross-sections a determination of electric multipole matrix elements is feasible.

The following theory describes multiple Coulomb excitation effects in neutron transfer reactions. It is based upon a semiclassical method and is a generalization of the theory of multiple Coulomb excitation by Alder and Winther [3].

2. DWBA Treatment of the Neutron Transfer Reaction

Starting point of our semiclassical time-dependent perturbation method is the DWBA expression for the T-matrix describing the subcoulomb neutron transfer reaction. So, we summarize the basic formulae of this theory.

We consider reactions of the form

$$\underset{a_1}{(c_1+n)}+c_2 \rightarrow c_1+\underset{a_2}{(c_2+n)}$$

where a neutron, bound to c_1 in a state described by angular momentum, spin and radial quantum number $(l_1\, j_1\, n_1)$ is transferred to a target nucleus c_2, where it will be in a bound state $(l_2\, j_2\, n_2)$. The bound state (c_i+n) is denoted by a_i. We shall use latin letters for the spins and masses of the four nuclei, greek letters for the magnetic quantum numbers. The subscripts 1 and 2 stand for the projectile and target, respectively.

We are now interested in the T-matrix which describes the transition from the initial state $|a_1\,\alpha_1\,c_2\,\gamma_2\rangle$ to the final state $|c_1\,\gamma_1\,a_2\,\alpha_2\rangle$.

In the post representation, the DWBA expression for the T-matrix has been given by Buttle and Goldfarb [1] as

$$\begin{aligned}\langle c_1\,\gamma_1\,a_2\,\alpha_2|T|a_1\,\alpha_1\,c_2\,\gamma_2\rangle = \sqrt{4\pi}\sum_{\substack{j_1 l_1 \xi_1\\ j_2 l_2 \xi_2}} \Theta_{j_1 l_1}\Theta_{j_2 l_2}(-1)^{j_1+j_2-c_1-c_2+\alpha_1+\gamma_2-1/2}\\ *i^{l_1+l_2}N_{l_2}A_{l_1}\begin{pmatrix} j_1 & c_1 & a_1\\ \xi_1 & \gamma_1 & -\alpha_1\end{pmatrix}\begin{pmatrix} j_2 & c_2 & a_2\\ \xi_2 & \gamma_2 & -\alpha_2\end{pmatrix}\hat{j}_1\hat{j}_2\hat{a}_1\hat{a}_2\\ *\sum_{l\lambda}\hat{l}\begin{pmatrix} j_1 & j_2 & l\\ \tfrac{1}{2} & -\tfrac{1}{2} & 0\end{pmatrix}\begin{pmatrix} j_1 & j_2 & l\\ -\xi_1 & \xi_2 & \lambda\end{pmatrix}T_{l\lambda}.\end{aligned} \tag{1}$$

The sum over the angular momentum l is restricted by the selection rules

$$\begin{aligned}&|l_1-l_2|\leqslant l\leqslant l_1+l_2,\\ &|j_1-j_2|\leqslant l\leqslant j_1+j_2,\\ &(-1)^l=(-1)^{l_1+l_2}.\end{aligned} \tag{2}$$

By $\Theta_{j_1 l_1}$ and $\Theta_{j_2 l_2}$, we denote the spectroscopic factors of the corresponding neutron state in the projectile and target, respectively. The symbol $\hat{j}$ is used for $(2j+1)^{1/2}$.

For the neutron wave functions, the definition

$$\Psi_{l\lambda}(\hat{r}) = i^l u_l(r)\, Y_{l\lambda}(\hat{r}) \tag{3}$$

has been used. Asymptotically, the real radial wave function $u_l(r)$ behaves like a spherical McDonald function $k_l(\kappa r)$ and its normalization N_l is defined by

$$N_l = \lim_{r\to\infty} (u_l(r)/k_l(\kappa r)). \tag{4}$$

The bound state wave number κ is connected with the neutron binding energy B by

$$\kappa = \left(\frac{2n^*|B|}{\hbar^2}\right)^{1/2}, \tag{5}$$

where n^* is the reduced mass of the neutron and the corresponding nuclear core c.

The form factor A_{l_1} is defined by

$$A_{l_1} = \int i_{l_1}(\kappa_2 r)\, V_{c_1 n}(r)\, u_{l_1}(r)\, r^2\, dr \tag{6}$$

Here, $V_{c_1 n}$ is the interaction potential between the neutron and the projectile core c_1.

By $i_l(x)$, we denote the modified spherical Bessel function

$$i_l(x) = \left(\frac{\pi}{2x}\right)^{1/2} I_{l+1/2}(x). \tag{7}$$

The quantity $T_{l\lambda}$ describes the kinematics of the reaction and is given by

$$T_{l\lambda} = \int d^3 r \chi^{(-)*}(\vec{k}_f, \vec{r}_f)\, k_l(\kappa_2 r)\, Y_{l\lambda}(\hat{r})\, \chi^{(+)}(\vec{k}_i, \vec{r}_i). \tag{8}$$

By $\chi^{(\pm)}(\vec{k}, \vec{r})$, we denote the Coulomb distorted wave functions which describe the relative motion of projectile and target in the entrance and exit channel, respectively. They are given by

$$\chi^{(+)}(\vec{k}_i, \vec{r}) = e^{-(\pi/2)\eta_i}\, \Gamma(1 + i\eta_i)\, e^{i\vec{k}_i\vec{r}}\, {}_1F_1(-i\eta_i, 1; i(k_i r - \vec{k}_i \vec{r})) \tag{9}$$

and

$$\chi^{(-)}(\vec{k}_f, \vec{r}) = e^{-(\pi/2)\eta_f}\, \Gamma(1 - i\eta_f)\, e^{i\vec{k}_f\vec{r}}\, {}_1F_1(i\eta_f, 1; -i(k_f r - \vec{k}_f \vec{r})). \tag{10}$$

Here, we have specified the scattering state of the projectile by its asymptotic momenta $\hbar\vec{k}_i$ and $\hbar\vec{k}_f$ before and after the collision. As usual, the dimensionless parameters η_i and η_f are defined by

$$\eta_{i,f} = \frac{Z_1 Z_2 e^2 m^*_{i,f}}{\hbar^2 k_{i,f}}. \tag{11}$$

By m_i^*, m_f^* we have specified the reduced masses in the entrance and exit channel

$$m_i^* = \frac{a_1 c_2}{a_1 + c_2}, \quad m_f^* = \frac{a_2 c_1}{a_1 + c_2}. \tag{12}$$

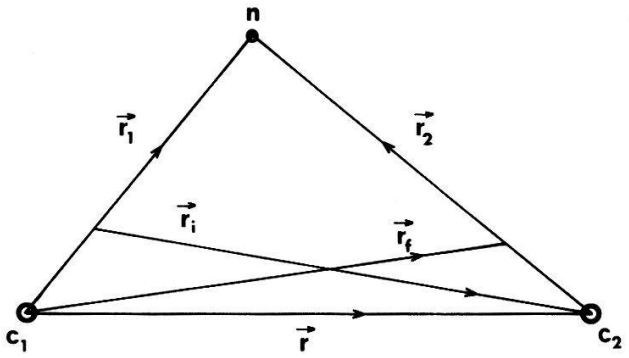

Figure 2
The coordinate system.

Z_1 and Z_2 denote the projectile and the target charge. Due to the mass transfer, we have to use different centre of mass coordinate systems in the two channels. In Figure 2 we show the connection between the various vectors employed in equation (8). They are related as follows

$$\vec{r}_2 = \vec{r}_1 - \vec{r}, \quad \vec{r}_i = \vec{r} - \frac{n}{a_1}\vec{r}_1 \tag{13}$$

and

$$\vec{r}_f = \frac{c_2}{a_2}\vec{r} + \frac{n}{a_2}\vec{r}_1. \tag{14}$$

The factorization of the T-matrix into a structure-dependent form factor A_{l_1} and a kinematics-dependent integral $T_{l\lambda}$ depends upon two approximations made:

i) The exact neutron wave function in the target $i^{l_2} u_{l_2}(r_2)\, Y_{l_2\lambda_2}(\hat{r}_2)$ can be replaced by its asymptotic form $N_{l_2} i^{l_2} k_{l_2}(\kappa_2 r_2)\, Y_{l_2\lambda_2}(\hat{r}_2)$. By means of an addition theorem this can be expressed in terms of products $k_l(\kappa_2 r)\, i_{l_1}(\kappa_2 r_1)\, Y_{l\lambda}(\hat{r})\, Y_{l_1\lambda_1}(\hat{r}_1)$ [1].

ii) The recoil effects which come from the change of the centre of mass coordinate system from the entrance to the exit channel, can be accounted for by approximating $\vec{r}_i$ and $\vec{r}_f$ as

$$\vec{r}_i = \left(1 - \frac{n}{a_1}\frac{R_1}{d}\right)\vec{r}, \quad \vec{r}_f = \left(\frac{c_2}{a_2} + \frac{n}{a_2}\frac{R_1}{d}\right)\vec{r} \tag{15}$$

where R_1 is the radius of the projectile core c_1 and d is a symmetrized classical distance of closest approach given by

$$d = \frac{Z_1 Z_2 e^2}{2\hbar^2}\left(\frac{m_i^*}{k_i^2} + \frac{m_f^*}{k_f^2}\right)\left(1 + \sin^{-1}\frac{\vartheta}{2}\right). \tag{16}$$

This expression is discussed in [4] and [5]. This approximation follows the idea that the main contribution to the T-matrix comes from the classical turning point, where the system is in a configuration in which the neutron lies in a straight line between the projectile and the target core [4]. By ϑ we denote the centre of mass scattering angle.

As the Coulomb function $\chi^{(\pm)}$ depends only on the scalar product of $\vec{k}$ and $\vec{r}$, it is possible to introduce new wave numbers $\vec{k}_i^*$, $\vec{k}_f^*$

$$\vec{k}_i^* = \vec{k}_i \left(1 - \frac{n}{a_1}\frac{R_1}{d}\right), \quad \vec{k}_f^* = \vec{k}_f \left(\frac{c_2}{a_2} + \frac{n}{a_2}\frac{R_1}{d}\right) \tag{17}$$

and to rewrite the integral $T_{l\lambda}$ as

$$T_{l\lambda} = \int d^3 r \chi^{(-)*}(\vec{k}_f^*, \vec{r})\, k_l(\kappa_2 r)\, Y_{l\lambda}(\hat{r})\, \chi^{(+)}(\vec{k}_i^*, \vec{r}) \tag{18}$$

depending on the vector $\vec{r}$ only. These approximations have been discussed by Buttle and Goldfarb [4].

An exact expression for the quantity $T_{l\lambda}$ has been given by Trautmann and Alder [6]. They have shown that for large values of the parameter η ($\eta > \sim 10$), it is possible to express $T_{l\lambda}$ as an integral along the classical hyperbolic trajectory, on which the projectile moves in the repulsive Coulomb field of the target nucleus. Their result can be written

$$T_{l\lambda} = \pi \frac{\eta}{k_{if}^2} a_{if} \sin^{-2}\frac{\vartheta}{2} \int_{-\infty}^{+\infty} e^{i(\delta_{fl}+\xi_{fl})\epsilon \sinh w + i\xi_{fl} w}$$

$$*(\epsilon \cosh w + 1)\, k_l(\kappa_2 r_p(w))\, Y_{l\lambda}(\vartheta_p(w), \varphi_p(w))\, dw. \tag{19}$$

The polar coordinates $r_p(w)$, $\vartheta_p(w)$, $\varphi_p(w)$ define the momentary projectile position relative to the centre of mass of the target in a parametric representation, in which the radial coordinate $r_p(w)$ and time coordinate t are given by

$$r_p(w) = a_{if}(\epsilon \cosh w + 1), \tag{20}$$

$$t = \frac{a_{if}}{v_{if}}(\epsilon \sinh w + w). \tag{21}$$

The angular coordinates depend upon the orientation of the coordinate system and will be defined in Section 3.

The quantity $2a_{if}$ corresponds to a symmetrized distance of closest approach for backward scattering

$$a_{if} = \frac{Z_1 Z_2 e^2}{\hbar^2} \frac{\sqrt{m_i^* \cdot m_f^*}}{k_i k_f} \tag{22}$$

and the eccentricity ϵ is connected with the scattering angle ϑ by

$$\epsilon = \sin^{-1}\frac{\vartheta}{2}. \tag{23}$$

The symbols v_{if}, k_{if} and η_{if} are used to denote the geometric mean of the corresponding entrance and exit channel values of the relative velocity v_i, v_f and of the quantities k_i^*, k_f^* and η_i, η_f, respectively.

The Q-value dependence of the reaction [5, 7] is described by the parameters

$$\xi_{fi} = \eta_f - \eta_i \tag{24}$$

and

$$\delta_{fi} = \frac{k_i^* \eta_i - k_f^* \eta_f}{k_{if}}. \tag{25}$$

For neutron transfer reactions in the subcoulomb energy range, the parameters η_i and η_f are usually very large ($\eta \gtrsim 10$), especially when heavy ions are used as projectiles.

The quality of the semiclassical approximation is then very good, its error being less than a few per cent. Compared to the other failures of the description of this reaction, e.g. errors arising from unknown properties of the neutron-projectile potential $V_{c_1 n}$ and from the approximations that allow the factorization of the T-matrix elements, it appears that the additional error of the semiclassical approximation is negligible.

The differential transfer cross-section $(d\sigma/d\Omega)_T$ is connected with the T-matrix as follows

$$\left(\frac{d\sigma}{d\Omega}\right)_T = \frac{m_i^* m_f^*}{(2\pi\hbar^2)^2}\frac{k_f}{k_i}\frac{1}{(2a_1+1)(2c_2+1)}\sum_{\substack{\gamma_1\alpha_2\\ \alpha_1\gamma_2}} |\langle \alpha_2 \gamma_1 | T | \alpha_1 \gamma_2 \rangle|^2. \tag{26}$$

Like in the theory of Coulomb excitation, we can write $(d\sigma/d\Omega)_T$ as a product of a symmetrized Rutherford cross-section

$$\left(\frac{d\sigma_\cdot}{d\Omega}\right)_R = \frac{a_{if}^2}{4}\sin^{-4}\frac{\vartheta}{2} \tag{27}$$

and a quantity $P_{if}(\vartheta)$, which gives the neutron transfer probability for a collision, in which the projectile is scattered into the solid angle $d\Omega$,

$$\left(\frac{d\sigma}{d\Omega}\right)_T = \left(\frac{d\sigma}{d\Omega}\right)_R P_{if}(\vartheta). \tag{28}$$

The probability $P_{if}(\vartheta)$ can be written as

$$P_{if} = \frac{1}{(2a_1+1)(2c_2+1)}\sum_{\substack{\alpha_1\gamma_2\\ \alpha_2\gamma_1}} |\langle \alpha_2 \gamma_1 | \tau | \alpha_1 \gamma_2 \rangle|^2 \tag{29}$$

where, according to [1, 26], the transition amplitudes $b_{if} = \langle \alpha_2 \gamma_1 | \tau | \alpha_1 \gamma_2 \rangle$ are given by

$$\begin{aligned} b_{if} = \langle \alpha_2 \gamma_1 | \tau | \alpha_1 \gamma_2 \rangle = {} & \sum_{\substack{j_1 l_1 \xi_1\\ j_2 l_2 \xi_2}} \Psi_{if}(j_1 l_1 j_2 l_2)\, i^{l_1+l_2} \\ & * (-1)^{j_1+j_2+\alpha_2+\gamma_1-c_1-c_2-1/2} \begin{pmatrix} j_1 & c_1 & a_1 \\ \xi_1 & \gamma_1 & -\alpha_1 \end{pmatrix} \begin{pmatrix} j_2 & c_2 & a_2 \\ \xi_2 & \gamma_2 & -\alpha_2 \end{pmatrix} \\ & * \sum_{l\lambda} \hat{l} \begin{pmatrix} j_1 & j_2 & l \\ \tfrac{1}{2} & -\tfrac{1}{2} & 0 \end{pmatrix} \begin{pmatrix} j_1 & j_2 & l \\ -\xi_1 & \xi_2 & \lambda \end{pmatrix} \int_{-\infty}^{+\infty} \mathcal{H}_{l\lambda}(\epsilon, \delta_{fi}, \rho_{fi}, w)\, e^{i\xi_{fi}(\epsilon \sinh w + w)}\, dw \end{aligned} \tag{30}$$

We have used the definitions

$$\mathscr{H}_{l\lambda}(\epsilon, \delta_{fi}, \rho_{fi}, w) = e^{i\delta_{fi}\epsilon \sinh w} k_l(\rho_{fi}(\epsilon \cosh w + 1)) \\ *(\epsilon \cosh w + 1) Y_{l\lambda}(\vartheta(w), \varphi(w)) \tag{31}$$

and

$$\rho_{fi} = \kappa_2 \; a_{fi}. \tag{32}$$

The dimensionless parameter

$$\Psi_{fi}(j_1 l_1 j_2 l_2) = \frac{a_{if}}{\hbar v_{if}} \sqrt{\frac{k_f}{k_i}} \sqrt{4\pi}\, \hat{j}_1 \hat{j}_2 \hat{a}_1 \hat{a}_2 \\ *\Theta_{j_1 l_1} \Theta_{j_2 l_2} A_{l_1} N_{l_2} \tag{33}$$

is a measure of the transfer coupling strength. The coupling functions $\mathscr{H}_{l\lambda}(\epsilon, \delta, \rho, w)$ describe how the transition amplitudes are being built up during the collision.

3. Virtual Coulomb Excitation Occurring in Transfer Reactions

We want to give a semiclassical description of neutron transfer reactions including virtual Coulomb excitation effects in both the projectile and the target nucleus.

In a time-dependent picture, the reaction is described by the time-dependent amplitudes of all the nuclear states involved, i.e. by the states of the projectiles and the target in both the entrance and exit channels. We introduce the free entrance and exit channel Hamiltonians $\mathscr{H}^{(0)}_{\text{ent}}$ and $\mathscr{H}^{(0)}_{\text{exit}}$ given by

$$\mathscr{H}^{(0)}_{\text{ent}} = \mathscr{H}^{(0)}_{c_2} + \mathscr{H}^{(0)}_{a_1} \tag{34}$$

and

$$\mathscr{H}^{(0)}_{\text{exit}} = \mathscr{H}^{(0)}_{a_2} + \mathscr{H}^{(0)}_{c_1}. \tag{35}$$

The free nuclear Hamiltonians we have introduced above define the following Schroedinger equations:

i) for the target in the entrance channel

$$\mathscr{H}^{(0)}_{c_2} |c_2 \gamma_2\rangle = E_{c_2} |c_2 \gamma_2\rangle \tag{36}$$

and in the exit channel

$$\mathscr{H}^{(0)}_{a_2} |a_2 \alpha_2\rangle = E_{a_2} |a_2 \alpha_2\rangle \tag{37}$$

ii) for the projectile in the entrance channel

$$\mathscr{H}^{(0)}_{a_1} |a_1 \alpha_1\rangle = E_{a_1} |a_1 \alpha_1\rangle \tag{38}$$

and in the exit channel

$$\mathscr{H}^{(0)}_{c_1} |c_1 \gamma_1\rangle = E_{c_1} |c_1 \gamma_1\rangle. \tag{39}$$

The notation for the energy eigenvalues employed is clear. The Schroedinger equations for $\mathscr{H}^{(0)}_{\text{ent}}$ and $\mathscr{H}^{(0)}_{\text{exit}}$ have the following form

$$\mathscr{H}^{(0)}_{\text{ent}} |c_2 \gamma_2 a_1 \alpha_1\rangle = (E_{c_2} + E_{a_1}) |c_2 \gamma_2 a_1 \alpha_1\rangle \tag{40}$$

and similarly for the exit channel

$$\mathscr{H}^{(0)}_{\text{exit}} |a_2 \alpha_2 c_1 \gamma_1\rangle = (E_{a_2} + E_{c_1}) |a_2 \alpha_2 c_1 \gamma_1\rangle. \tag{41}$$

Formally, we can construct a free Hamiltonian $\mathscr{H}_0$ of the form

$$\mathscr{H}_0 = \begin{pmatrix} \mathscr{H}^{(0)}_{\text{ent}} & 0 \\ 0 & \mathscr{H}^{(0)}_{\text{exit}} \end{pmatrix}. \tag{42}$$

Its eigenstates $\phi^{(l)}_{ik}$ either belong to the entrance channel ($l = 1$) or to the exit channel ($l = 2$). They satisfy the Schroedinger equation

$$\mathscr{H}_0 \phi^{(l)}_{ik} = E^{(l)}_{ik} \phi^{(l)}_{ik} \tag{43}$$

and are defined by

$$\phi^{(1)}_{ik} = \begin{pmatrix} |a_1^{(i)} \alpha_1^{(i)} c_2^{(k)} \gamma_2^{(k)}\rangle \\ 0 \end{pmatrix}, \tag{44}$$

$$\phi^{(2)}_{ik} = \begin{pmatrix} 0 \\ |c_1^{(i)} \gamma_1^{(i)} a_2^{(k)} \alpha_2^{(k)}\rangle \end{pmatrix}, \tag{45}$$

while the eigenvalues are given by

$$E^{(1)}_{ik} = E_{a_1^{(i)}} + E_{c_2^{(k)}}, \tag{46}$$

$$E^{(2)}_{ik} = E_{c_1^{(i)}} + E_{a_2^{(k)}}. \tag{47}$$

The total Hamiltonian describing our transfer reaction can be written

$$\mathscr{H} = \mathscr{H}_0 + \mathscr{H}_{\text{int}}(t). \tag{48}$$

The interaction Hamiltonian $\mathscr{H}_{\text{int}}(t)$ consists of four parts: one—$\mathscr{H}_T^{\text{ent}\to\text{exit}}$—describing the neutron transfer, one—$\mathscr{H}_T^{\text{exit}\to\text{ent}}$—for the reabsorption of a neutron, and two parts —$\mathscr{H}^{\text{ent}}_{\text{CE}}$ and $\mathscr{H}^{\text{exit}}_{\text{CE}}$—responsible for the Coulomb excitation in the extrance and exit channel, respectively

$$\mathscr{H}_{\text{int}} = \begin{pmatrix} \mathscr{H}^{\text{ent}}_{\text{CE}} & \mathscr{H}_T^{\text{exit}\to\text{ent}} \\ \mathscr{H}_T^{\text{ent}\to\text{exit}} & \mathscr{H}^{\text{exit}}_{\text{CE}} \end{pmatrix}. \tag{49}$$

The total wave function of the system Ψ satisfies a time-dependent Schroedinger equation of the form

$$i\hbar\dot{\Psi} = \mathscr{H}\Psi. \tag{50}$$

It is usual to change from the Schroedinger to the interaction picture by introducing a state vector

$$\chi = e^{(i/\hbar)\mathscr{H}_0 t}\, \Psi, \tag{51}$$

which for vanishing $\mathscr{H}_{\text{int}}(t)$, i.e. before and after the collision, is time independent. It satisfies the equation

$$i\hbar \frac{\partial}{\partial t} \chi = \mathscr{H}^{I}_{\text{int}}(t)\, \chi, \tag{52}$$

where

$$\mathscr{H}^{I}_{\text{int}}(t) = e^{(i/\hbar)\mathscr{H}_0 t}\, \mathscr{H}_{\text{int}}(t)\, e^{-(i/\hbar)\mathscr{H}_0 t} \tag{53}$$

is the interaction Hamiltonian in the interaction picture. Neglecting possible effects of non-orthogonality between the states $\phi^{(l)}_{ik}$ [8], the wave function χ can be written as a time-dependent superposition of the nuclear eigenstates $\phi^{(l)}_{ik}$

$$\chi(t) = \sum_{ikl} a^{(l)}_{ik}(t)\, \phi^{(l)}_{ik} \tag{54}$$

with

$$a^{(l)}_{ik} = \langle \phi^{(l)}_{ik} | \chi(t) \rangle. \tag{55}$$

Equation (52) may then be formulated as a set of coupled differential equations for the nuclear amplitudes

$$i\hbar \frac{\partial a^{(l)}_{ik}}{\partial t} = \sum_{\iota\kappa\lambda} \langle \phi^{(l)}_{ik} | \mathscr{H}_{\text{int}}(t) | \phi^{(\lambda)}_{\iota\kappa} \rangle \exp\left[\frac{i(E^{(l)}_{ik} - E^{(\lambda)}_{\iota\kappa})\, t}{\hbar}\right] a^{(\lambda)}_{\iota\kappa}(t). \tag{56}$$

This set of coupled differential equations must be solved subject to the initial conditions appropriate to the particular experimental situation.

For unpolarized targets and projectiles, these conditions have the form

$$a^{(l)}_{ik}(t = -\infty, i_0\, k_0) = \delta_{ii_0} \delta_{kk_0} \delta_{l1}. \tag{57}$$

where i_0 and k_0 refer to the magnetic substates of the projectile and target ground states in the entrance channel.

The time-dependent interaction matrix elements $\langle \phi^{(l)}_{ik} | \mathscr{H}_{\text{int}}(t) | \phi^{(\lambda)}_{\iota\kappa} \rangle$ are defined such that the first-order results obtained from (56) are equal to the transition amplitudes b_{if}, defined in (30), namely

$$b_{if} = \frac{1}{i\hbar} \int_{-\infty}^{+\infty} \langle \phi^{(l)}_{ik} | \mathscr{H}_{\text{int}}(t) | \phi^{(\lambda)}_{\iota\kappa} \rangle \exp\left[\frac{i(E^{(l)}_{ik} - E^{(\lambda)}_{\iota\kappa})\, t}{\hbar}\right] dt. \tag{58}$$

This is achieved by defining the time-dependent interaction matrix element as the Fourier transform of the corresponding transition amplitude, which is a function of the nuclear transition frequency $\omega = (E_f - E_i)/\hbar$,

$$\langle f | \mathscr{H}_{\text{int}}(t) | i \rangle = \frac{i\hbar}{2\pi} \int_{-\infty}^{+\infty} b_{if}(\omega)\, e^{-i\omega t}\, d\omega. \tag{59}$$

In the following, we shall simplify the system of differential equations (56) considerably by neglecting the term $\mathscr{H}_T^{\text{exit}\to\text{ent}}$. This means that we do not take into account the

possibility that a neutron, already transferred to the target, can be reabsorbed by the projectile.

This approximation is justified by the following argument: second-order processes, corresponding to a stripping followed by a pick-up of a neutron, are in their effect equivalent to the simultaneous Coulomb excitation of both the projectile and the target, but give a negligible contribution to the excitation amplitudes due to the smallness of the transfer coupling strength.

Furthermore, as the target and the projectile are Coulomb excited independently of one another [9], it is now possible to factorize the entrance channel amplitudes

$$a_{ik}^{(1)}(t, i_0, k_0) = N_i^P(t, i_0)\, N_k^T(t, k_0). \tag{60}$$

where the amplitudes N_i^P and N_k^T refer to the projectile state $|i\rangle$ and to the target state $|k\rangle$, respectively. For the exit channel amplitudes we shall use the symbol

$$X_{ik}(t, i_0, k_0) = a_{ik}^{(2)}(t, i_0 k,) \tag{61}$$

where we explicitly specify the initial conditions at $t = -\infty$. Introducing instead of the time variable t, the previously (21) defined parameter w, the equations (56) now take the form

$$\frac{d}{dw} N_i^{P,T}(w, i_0) = -i \sum_k \langle i|\mathscr{H}_{\mathrm{CE}}^{P,T}(w)|k\rangle\, e^{i\xi_{ik}(\epsilon \sinh w + w)}\, N_k^{P,T}(w, i_0). \tag{62}$$

$$\begin{aligned}\frac{d}{dw} X_{ik}(w, i_0\, k_0) = &-i \sum_{i'k'} \langle ik|\mathscr{H}_T(w)|i'\, k'\rangle\, e^{i\xi_{ik\, i'k'}(\epsilon \sinh w + w)}\, N_{i'}^P(w, i_0)\, N_{k'}^T(w, k_0) \\ &-i \sum_{i'} \langle i|\mathscr{H}_{\mathrm{CE}}^P(w)|i'\rangle\, e^{i\xi_{ii'}(\epsilon \sinh w + w)}\, X_{i'k}(w, i_0\, k_0) \\ &-i \sum_{k'} \langle k|\mathscr{H}_{\mathrm{CE}}^T(w)|k'\rangle\, e^{i\xi_{kk'}(\epsilon \sinh w + w)}\, X_{ik'}(w, i_0\, k_0).\end{aligned} \tag{62}$$

The first set of these differential equations describes the Coulomb excitation of the projectile and target in the entrance channel. The second set consists of three terms, the first one describes the transfer interaction and plays the role of a source function (an inhomogeneity), while the last two terms give the Coulomb excitation of the projectile and target in the exit channel. Similar equations have been derived by Broglia and Winther [8].

If for the parameter ξ_{fi} the expression $\eta_f - \eta_i$ is used, instead of the semiclassical value $(E_f - E_i)\, a_{if}/\hbar v_{if}$, the transfer interaction matrix element can, according to (30) and (59), be written as

$$\begin{aligned}\langle \alpha_2 \gamma_1|\mathscr{H}_T(w)|\alpha_1 \gamma_2\rangle = &\sum_{\substack{j_1 l_1 \xi_1 \\ j_2 l_2 \xi_2}} \Psi_{fi}(j_1 l_1 j_2 l_2)(-1)^{j_1+j_2+\alpha_2+\gamma_1-c_1-c_2-1/2} \\ &*i^{l_1+l_2} \begin{pmatrix} j_1 & c_1 & a_1 \\ \xi_1 & \gamma_1 & -\alpha_1 \end{pmatrix} \begin{pmatrix} j_2 & c_2 & a_2 \\ \xi_2 & \gamma_2 & -\alpha_2 \end{pmatrix} \\ &\times \sum_{l\lambda} \hat{l} \begin{pmatrix} j_1 & j_2 & l \\ \frac{1}{2} & -\frac{1}{2} & 0 \end{pmatrix} \begin{pmatrix} j_1 & j_2 & l \\ -\xi_1 & \xi_2 & \lambda \end{pmatrix} \mathscr{H}_{l\lambda}(\epsilon, \delta_{fi}, \rho_{fi}, w).\end{aligned} \tag{63}$$

For $E2$-excitation, the Coulomb excitation Hamiltonian is given by [10]

$$\mathscr{H}_{\mathrm{CE}}^{P,T} = -\frac{4\pi}{5}\frac{Z_{1,2}\,e}{\hbar v_{if}\,a_{if}^2}\sum_{\mu}\frac{Y_{2\mu}(\vartheta_p(w),\varphi_p(w))}{(\epsilon\cosh w+1)}M(E2,\mu), \tag{64}$$

where for the electric multipole operator the definition

$$M(E\lambda,\mu) = i^{\lambda}\int r^{\lambda}Y_{\lambda\mu}(\vartheta,\varphi)\,\rho(\vec{r})\,d^3r \tag{65}$$

has been used. By $\rho(\vec{r})$, we denote the nuclear charge density operator.

For the numerical solution of our system of differential equations (62), we choose a focal coordinate system, whose x-axis is perpendicular to the plane of the orbit and whose z-axis coincides with the symmetry axis of the hyperbolic trajectory, such that

$$\begin{aligned} x &= 0 \\ y &= a_{if}(\epsilon^2-1)^{1/2}\sinh w \\ z &= a_{if}(\cosh w+\epsilon). \end{aligned} \tag{66}$$

In this coordinate system, the interaction matrix elements have properties which lead to the following symmetry relation for the exit channel amplitudes

$$X_{\gamma_1\alpha_2}(w=\infty,\alpha_1,\gamma_2) = (-1)^{l+a_2+c_1-a_1-c_2}\,X_{-\gamma_1-\alpha_2}(w=\infty,-\alpha_1-\gamma_2), \tag{67}$$

where l is the transferred angular momentum. The differential cross-section for transfer to the final state $|f\rangle$ is obtained from the exit channel amplitudes at $w=\infty$,

$$\left(\frac{d\sigma_f}{d\Omega}\right)_T = \left(\frac{d\sigma}{d\Omega}\right)_R \frac{1}{(2a_1+1)(2c_2+1)}\sum_{\alpha_1\gamma_2\alpha_2\gamma_1}|X_{\alpha_2\gamma_1}(w=\infty,\alpha_1\gamma_2)|^2. \tag{68}$$

The sum extends over all magnetic substates $|\gamma_1\alpha_2\rangle$ of the final state $|f\rangle$ and over all initial polarizations $|\alpha_1\gamma_2\rangle$ of the initial state $|i\rangle$. The transfer cross-section now depends on the reduced $E2$-matrix elements M_{rs}

$$M_{rs} = \langle r\|M(E2)\|s\rangle, \tag{69}$$

which are defined by the relation

$$\langle a_r\,\alpha_r|\mathscr{M}(E\lambda,\mu)\,|a_s\,\alpha_s\rangle = (-1)^{a_r-\alpha_r}\begin{pmatrix} a_r & \lambda & a_s \\ -\alpha_r & \mu & \alpha_s\end{pmatrix}\langle a_r\|\mathscr{M}(E\lambda)\|a_s\rangle. \tag{70}$$

We define an excitation effect function $\phi_f(\vartheta)$, which measures the relative change of the cross-section for transfer to the state $|f\rangle$ due to the virtual excitation of intermediate states,

$$\frac{d\sigma_f}{d\Omega} = \frac{d\sigma_f^{(0)}}{d\Omega}(1+\phi_f(\vartheta)). \tag{71}$$

By $d\sigma_f^{(0)}$, we denote the pure transfer cross-section for vanishing $E2$-matrix elements.

This effect function can be determined by the numerical solution of the coupled differential equations (62). Its properties will be discussed in Section 4. For small values of the electric quadrupole matrix elements, ϕ_f can be approximated as a linear function of M_{rs},

$$\phi_f(\vartheta, M_{rs}) = \sum_z M_{iz}\, E_{izf}^{(\mathrm{ent})}(\vartheta) + \sum_z M_{zf}\, E_{izf}^{(\mathrm{exit})}(\vartheta). \tag{72}$$

The functions $E_{izf}^{(\mathrm{ent})}(\vartheta)$ and $E_{izf}^{(\mathrm{exit})}(\vartheta)$ give the linearized effect on the cross-section for transfer to the state $|f\rangle$ due to the excitation of an intermediate state $|z\rangle$ in the entrance and exit channel, respectively. An analytical expression for these functions can be obtained by solving equation (62) to first order in the Coulomb excitation Hamiltonian $\mathscr{H}_{\mathrm{CE}}$.

The second-order amplitude $b_{if}^{(2)}$ for the transition from an initial state $|i\rangle$ to a final state $|f\rangle$ contains, apart from the first-order transfer amplitude $b_{if}^{T} = \langle f|\tau|i\rangle$ (30), two different second-order terms $b_{izf}^{(\mathrm{ent})}$ and $b_{izf}^{(\mathrm{exit})}$, corresponding to indirect transitions via an intermediate state $|z\rangle$, namely

$$b_{if}^{(2)} = b_{if}^{T} + \sum_z b_{izf}^{(\mathrm{ent})} + \sum_z b_{izf}^{(\mathrm{exit})} \tag{73}$$

with

$$b_{izf}^{(\mathrm{ent})} = \frac{1}{(i\hbar)^2} \int_{-\infty}^{+\infty} dt\, e^{i\omega_{fz}t} \langle f|\mathscr{H}_T(t)|z\rangle \int_{-\infty}^{t} dt' \langle z|\mathscr{H}_{\mathrm{CE}}^{\mathrm{ent}}(t')|i\rangle\, e^{i\omega_{zi}t'} \tag{74}$$

and

$$b_{izf}^{(\mathrm{exit})} = \frac{1}{(i\hbar)^2} \int_{-\infty}^{+\infty} dt\, e^{i\omega_{fz}t} \langle f|\mathscr{H}_{\mathrm{CE}}^{\mathrm{exit}}(t)|z\rangle \int_{-\infty}^{t} dt' \langle z|\mathscr{H}_T(t')|i\rangle\, e^{i\omega_{zi}t'}. \tag{75}$$

The time-ordered double integrals in (74) and (75) can be transformed into integrals over first-order transition amplitudes at off-shell transition frequencies [10],

$$b_{izf}^{(\mathrm{ent})} = -\lim_{\delta\to 0^+} \frac{1}{2\pi i} \int_{-\infty}^{+\infty} \frac{d\omega}{\omega + i\delta}\, b_{iz}^{\mathrm{CE}}(\omega_{iz} + \omega)\, b_{zf}^{T}(\omega_{fz} - \omega) \tag{76}$$

and

$$b_{izf}^{(\mathrm{exit})} = -\lim_{\delta\to 0^+} \frac{1}{2\pi i} \int_{-\infty}^{+\infty} \frac{d\omega}{\omega + i\delta}\, b_{iz}^{T}(\omega_{iz} + \omega)\, b_{zf}^{\mathrm{CE}}(\omega_{fz} - \omega). \tag{77}$$

The first-order transition amplitudes for Coulomb excitation and neutron transfer are denoted by b_{if}^{CE} and b_{if}^{T}, respectively.

This leads to a transfer cross-section of the following form

$$\frac{d\sigma_f}{d\Omega} = \left(\frac{d\sigma}{d\Omega}\right)_R \sum |b_{if}^{T} + \sum_z b_{izf}^{(\mathrm{ent})} + \sum_z b_{izf}^{(\mathrm{exit})}|^2 \tag{78}$$

or, neglecting terms quadratic in the $E2$-matrix elements

$$\frac{d\sigma_f}{d\Omega} = \left(\frac{d\sigma}{d\Omega}\right)_R \sum \left\{ |b_{if}^{T}|^2 + 2\mathrm{Re}\, b_{if}^{T*} \left[\sum_z b_{izf}^{(\mathrm{ent})} + \sum_z b_{izf}^{(\mathrm{exit})} \right] \right\} \tag{79}$$

where the symbol $\sum$ indicates summing over the magnetic substrates of the final state $|f\rangle$ and averaging over the initial polarizations.

If in the entrance channel only projectile excitation and in the exit channel only target excitation is taken into account, this leads to the following expressions for the functions $E_{izf}^{(\mathrm{ent})}$ and $E_{izf}^{(\mathrm{exit})}$ [11]

$$E_{izf}^{(\mathrm{ent})} = (-1)^{c_1+a_z-j_z}\, i^{l_1-l_z}\, \hat{j}_1^2 \frac{4\pi Z_2 e}{5\hbar v_{iz} a_{iz}^2} \frac{v_z}{v_i} M_{iz}^P \frac{\psi_{zf}(j_z l_z j_2 l_2)}{\psi_{if}(j_1 l_1 j_2 l_2)}$$

$$* \sum_{ll'} \left[\hat{l}\hat{l}' \begin{pmatrix} j_1 & j_2 & l \\ \frac{1}{2} & -\frac{1}{2} & 0 \end{pmatrix} \begin{pmatrix} j_z & j_2 & l' \\ \frac{1}{2} & -\frac{1}{2} & 0 \end{pmatrix} \begin{Bmatrix} j_z & 2 & j_1 \\ a_1 & c_1 & a_2 \end{Bmatrix} \begin{Bmatrix} l' & 2 & l \\ j_1 & j_2 & j_z \end{Bmatrix} \right.$$

$$\left. * \sum_m (-1)^m Y_{lm}\left(\frac{\pi}{2}, 0\right) I_{lm}^T(\vartheta, \xi_{fi}, \delta_{fi}, \rho_{fi})\, \beta_{l-m}(l', \xi_{zi}, \xi_{fz}, \delta_{fz}, \rho_{fz}, \vartheta) \right]$$

$$* \left(\sum_\lambda \begin{pmatrix} j_1 & j_2 & \lambda \\ \frac{1}{2} & -\frac{1}{2} & 0 \end{pmatrix}^2 B_\lambda(\vartheta, \xi_{fi}, \delta_{fi}, \rho_{fi}) \right)^{-1} \tag{80}$$

and

$$E_{izf}^{(\mathrm{exit})} = (-1)^{c_2+a_2-j_1}\, i^{l_2-l_z}\, \hat{j}_2^2 \frac{4\pi Z_2 e}{5\hbar v_{zf} a_{zf}} \frac{\rho_{fi}}{\rho_{fz}} M_{zf} \frac{\psi_{iz}(j_1 l_1 j_z l_z)}{\psi_{if}(j_1 l_1 j_2 l_2)}$$

$$* \sum_{ll'} \left[\hat{l}\hat{l}' \begin{pmatrix} j_1 & j_2 & l \\ \frac{1}{2} & -\frac{1}{2} & 0 \end{pmatrix} \begin{pmatrix} j_1 & j_z & l' \\ \frac{1}{2} & -\frac{1}{2} & 0 \end{pmatrix} \begin{Bmatrix} j_z & 2 & j_z \\ a_2 & c_2 & a_z \end{Bmatrix} \begin{Bmatrix} l' & 2 & l \\ j_2 & j_1 & j_z \end{Bmatrix} \right.$$

$$\left. * \sum_m (-1)^m Y_{lm}\left(\frac{\pi}{2}, 0\right) I_{lm}^T(\vartheta, \xi_{fi}, \delta_{fi}, \rho_{fi})\, \beta_{l-m}(l', \xi_{fz}, \xi_{zi}, \delta_{zi}, \rho_{zi}, \vartheta) \right]$$

$$* \left(\sum_\lambda \begin{pmatrix} j_1 & j_2 & l \\ \frac{1}{2} & -\frac{1}{2} & 0 \end{pmatrix}^2 B_\lambda(\vartheta, \xi_{fi}, \delta_{fi}, \rho_{fi}) \right)^{-1}. \tag{81}$$

Here, we have introduced the orbital integrals of Coulomb excitation $I_{\lambda\mu}^{\mathrm{CE}}(\vartheta, \xi)$ [10] and those of neutron transfer $I_{lm}^T(\vartheta, \xi, \delta, \rho)$ [5], defined by

$$I_{\lambda\mu}^{\mathrm{CE}}(\vartheta, \xi) = \int_{-\infty}^{+\infty} e^{i\xi(\epsilon \sinh w + w)} \frac{(\cosh w + \epsilon + i(\epsilon^2 - 1)^{1/2} \sinh w)^\mu}{(\epsilon \cosh w + 1)^{\lambda+\mu}}\, dw \tag{82}$$

and

$$I_{lm}^T(\vartheta, \xi, \delta, \rho) = \int_0^\infty dw\, k_l(\rho(\epsilon \cosh w + 1))\, \rho(\epsilon \cosh w + 1)$$

$$* \cos\left((\xi + \delta)\, \epsilon \sinh w + \xi w + m \operatorname{arctg} \frac{(\epsilon^2 - 1)^{1/2} \sinh w}{\cosh w + \epsilon} \right). \tag{83}$$

The function B_λ is given by

$$B_\lambda(\vartheta, \xi, \delta, \rho) = \sum_\mu \left| Y_{\lambda\mu}\left(\frac{\pi}{2}, 0\right) I^T_{\lambda\mu}(\vartheta, \xi, \delta, \rho) \right|^2, \tag{84}$$

and β_{lm} is defined in terms of principal value integrals

$$\beta_{lm}(l', \xi_1, \xi_2, \delta, \rho, \vartheta) = \sum_{m'\mu'} \begin{pmatrix} l' & 2 & l \\ m' & \mu' & m \end{pmatrix} Y_{l'm'}\left(\frac{\pi}{2}, 0\right) Y_{2\mu'}\left(\frac{\pi}{2}, 0\right)$$

$$* \frac{1}{\pi} P \int_{-\infty}^{+\infty} \frac{d\xi}{\xi} I^T_{l'm'}(\vartheta, \xi_2 + \xi, \delta, \rho)\, I^{\mathrm{CE}}_{2\mu'}(\vartheta, \xi_1 - \xi). \tag{85}$$

4. Numerical Results and Discussion

In this section, we present some numerical results of the Coulomb excitation effects in neutron transfer reactions. Due to the great number of nuclear and kinematical parameters on which the excitation effect functions depend, we have to confine our discussion to a few instructive examples. We limit ourselves to reactions in which the Coulomb excitation effects include only the excitation of the projectile in the entrance channel and of the target in the exit channel.

4.1 *Computation of form factors and normalization factors*

The radial neutron wave functions $u_l(r)$ (3) are determined by numerical solution of the radial Schroedinger equations, using for the potential V_{cn} a Woods–Saxon shape with radius $R_0 a^{1/3}$ and diffuseness d. For a given bound state, characterized by spin, angular momentum and radial quantum number, the depth V_0 of the potential is chosen such that the energy eigenvalue matches the experimental value of the neutron binding energy. For the sake of simplicity, no spin orbit potential has been included.

4.2 *Properties of the Excitation effect functions*

We will take the reaction ^{208}Pb(^{17}O, ^{16}O)^{209}Pb to serve us as a test case for the investigation of the various properties of the excitation effect functions (EEF) (71). To a very good approximation, in the entrance channel we only have the excitation of the $1/2^+$ state of ^{17}O at .871 MeV, whereas in the exit channel the main contributions arise from the excitation and de-excitation of the different ^{209}Pb levels. We study the EEF in the following ^{209}Pb states: $5/2^+$ at 1.56 MeV, $1/2^+$ at 2.01 MeV, $7/2^+$ at 2.47 MeV and $3/2^+$ at 2.52 MeV. Unless otherwise specified, the reaction is calculated at a laboratory energy of 70 MeV, corresponding to some 75% of the Coulomb barrier, and for the Woods–Saxon parameters, R_0 and d, values of 1.3 fm and .5 fm are used.

4.2.1 *Dependence of the EEF on the electric quadrupole matrix elements.* In Figure 3 the target EEF for backward scattering are plotted as functions of the electric quadrupole matrix elements. The same value x is used for all non-vanishing couplings between the four levels of ^{209}Pb. It can been seen that the deviations from linearity are quite small. In Figure 4 a similar plot shows the projectile EEF for backward

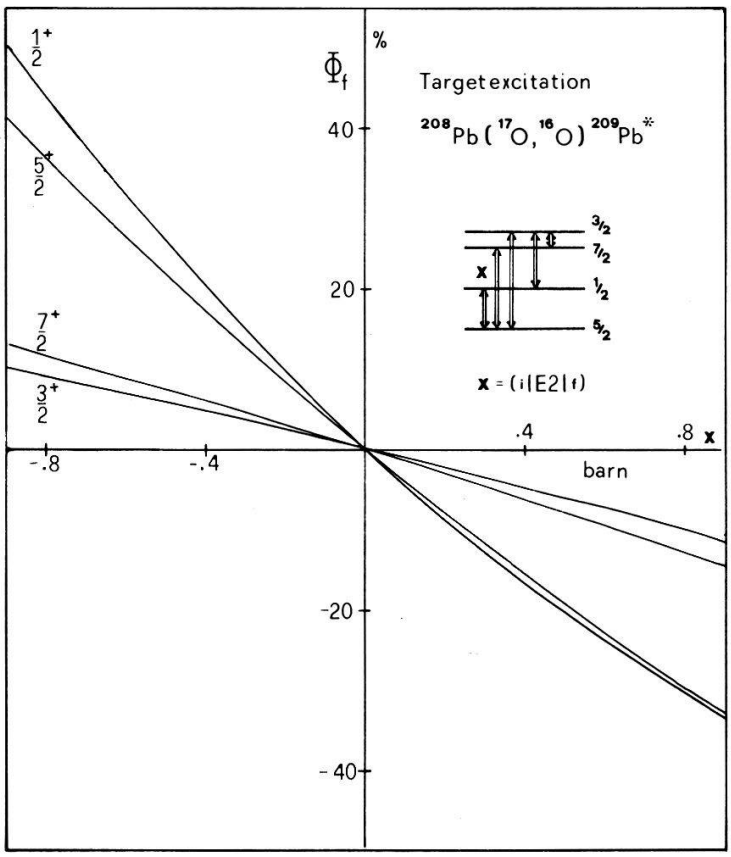

Figure 3
The target excitation effects are displayed as functions of the electric quadrupole couplings between the four states of ^{209}Pb. The same value x is used for all non-vanishing $E2$-matrix elements.

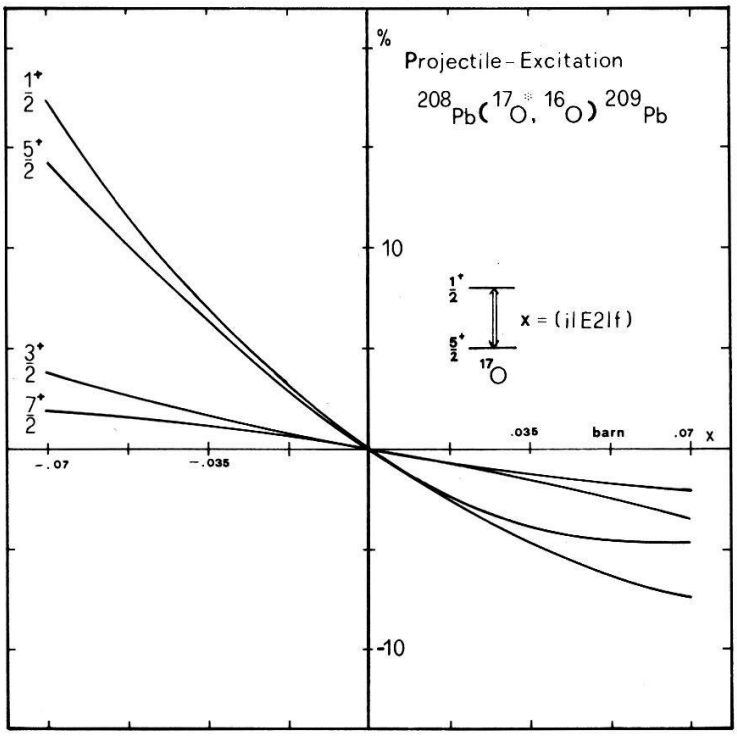

Figure 4
The projectile excitation effects in four levels of ^{209}Pb are plotted as functions of the $E2$-couplings between the states $5/2^+$ and $1/2^+$ in ^{17}O.

scattering as functions of the ^{17}O-quadrupole matrix elements

$$x = \langle 5/2^+ \| \mathcal{M}(E2) \| 1/2^+ \rangle = \langle 5/2^+ \| \mathcal{M}(E2) \| 5/2^+ \rangle.$$

Again, the EEF can approximately be represented as linear functions of x.

4.2.2. *Dependence of the EEF on the spectroscopic factors.* In Figure 5 the EEF $\Phi_{5/2}$ of the $5/2^+$ state of ^{209}Pb is shown as a function of the ratio R of the spectroscopic factors $\Theta_{1/2}$ and $\Theta_{5/2}$ of the $1/2^+$- and $5/2^+$-state of ^{209}Pb for different values of the $E2$ matrix elements $x_1 = \langle 5/2^+ \| \mathcal{M}(E2) \| 5/2^+ \rangle$ and $x_2 = \langle 5/2^+ \| \mathcal{M}(E2) \| 1/2^+ \rangle$.

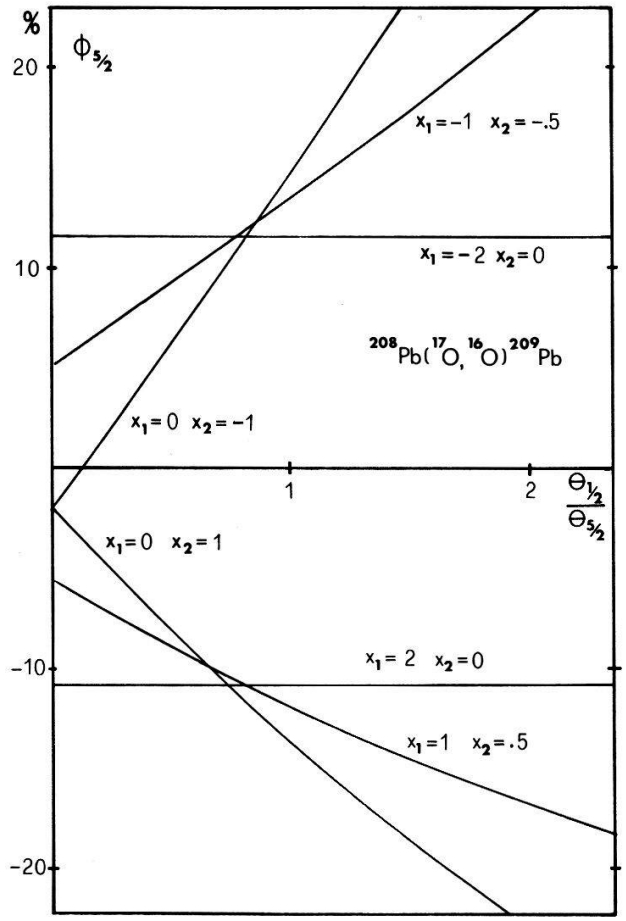

Figure 5
The target excitation effects in two levels of ^{209}Pb are shown as functions of the spectroscopic factors $\Theta_{1/2}$ and $\Theta_{5/2}$ for different values of the reduced matrix elements $x_1 = M^T_{5/2\,5/2}$ and $x_2 = M^T_{5/2\,1/2}$. The values are given in barn.

As suggested by equations (80, 81), the excitation effect should be a linear function of R and the effect, due to the reorientation of the 5/2 state, described by

$$x_1 = \langle 5/2^+ \| \mathcal{M}(E2) \| 5/2^+ \rangle, \quad x_2 = 0$$

should be independent of R. This is confirmed to a high degree of accuracy. Higher order terms, however, prevent the EEF for $x_1 = 0$ from passing through the origin.

In the same way, it has been found that the effects, due to the projectile excitation, are similarly linear functions of the ratio of the corresponding spectroscopic factors.

4.3. *Linear approximation of the EEF*

The results presented in Section 4.2, lead to the following approximation for the EEF

$$\phi_f(\vartheta, M_{rs}) = \sum_z \frac{\Theta_z^P}{\Theta_i^P} M_{iz}^P E_{zf}^P(\vartheta) + \sum_z \frac{\Theta_z^T}{\Theta_f^T} M_{zf}^T E_{zf}^T(\vartheta). \tag{86}$$

The functions $E_{zf}^P(\vartheta)$ ($E_{zf}^T(\vartheta)$) give the linearized excitation effect in the state $|f\rangle$, due to the indirect transition via the projectile-(target-) state $|z\rangle$ for a value of 1 barn

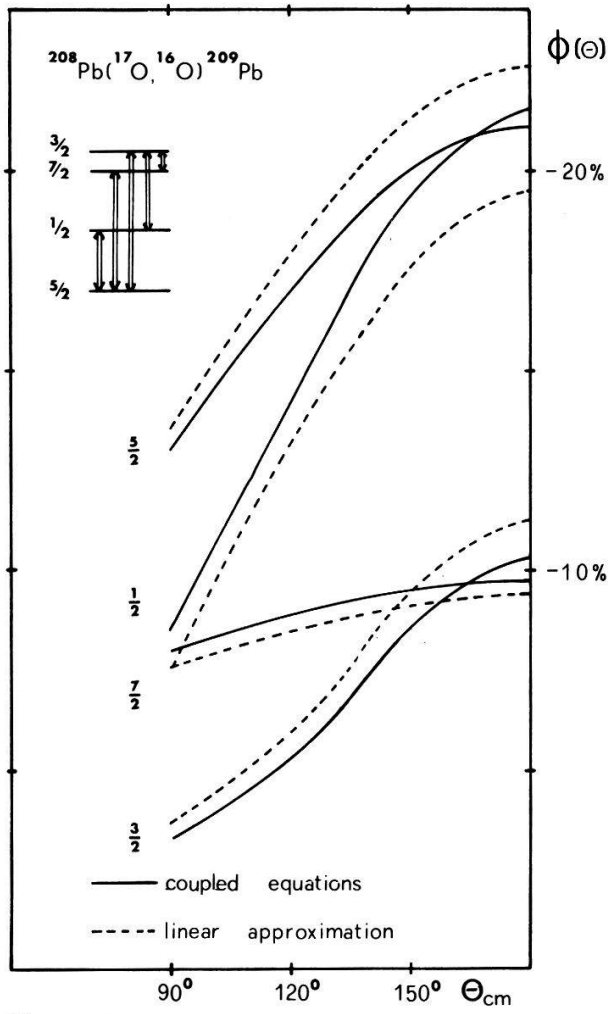

Figure 6

The target excitation effects, as obtained from the linear approximation (86), are compared to those determined by the exact numerical solution of the coupled equations (62). They are plotted as functions of the centre of mass scattering angle. For all non-vanishing $E2$-couplings the same value of $-.8$ barn is used.

for the quadrupole matrix element $M_{iz}^P(M_{zf}^T)$. In Figure 6 we show a comparison between the excitation effects obtained from the linear approximation (86) and those determined from the direct numerical solution of the differential equations (62). A value of $-.8$ barn has been used for all non-zero $E2$-matrix elements. The functions $E_{zf}^P(\vartheta)$ and $E_{zf}^T(\vartheta)$ have been computed by solving the differential equations (62) for different very small values ($\sim.01$ barn) of the electric quadrupole matrix elements.

4.4 *Dependence of the EEF on the parameters of the Woods–Saxon potential*

A study of equations (80) and (81) shows that the linearized excitation effects only depend on ratios between the transfer coupling parameters of different levels. While the magnitude of the form factors A_{l_1} strongly depends upon the values of the Woods–Saxon parameters R_0 and d, their ratio for different levels of the same nucleus remains approximately constant. The normalization factors show a similar behavior. The EEF should therefore not be very sensitive to the specific values used for R_0 and d. This is confirmed by the numerical results. In Figure 7 we show, as an example, the EEF $E^T_{1/2\,5/2}$ ($\vartheta = 180°$) for a wide range of values of the parameters R_0 and d.

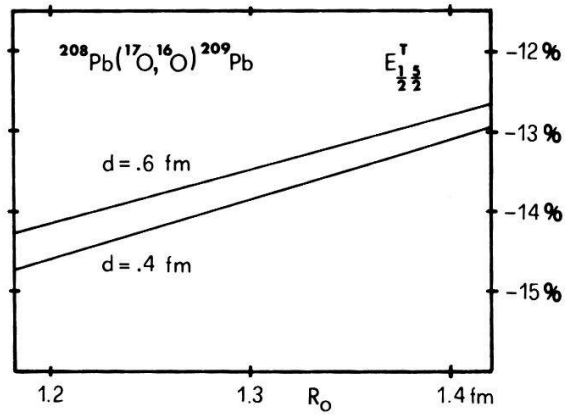

Figure 7
The excitation effect function $E^T_{1/2\,5/2}$ ($\vartheta = 180°$) as a function of the Woods–Saxon parameters R_0 and d.

4.5. *Dependence of the EEF on the laboratory energy*

The dependence of the EEF on the bombarding energy is of complex structure. No simple rules seem to be applicable, since the excitation effects depend in a complicated way on the combination of the angular momentum transfer values occurring in the transition.

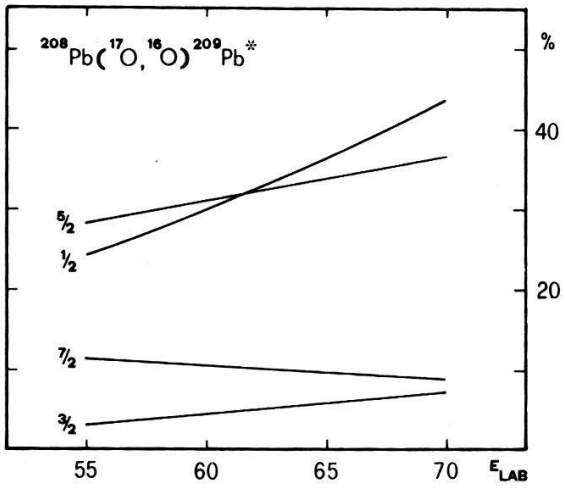

Figure 8
The energy dependence of the target excitation effects in four levels of ^{209}Pb. A value of $-.8$ barn is used for all non-vanishing $E2$-couplings.

In Figure 8, we show the energy dependence of the target excitation effects in the four levels of ^{209}Pb. For all reduced quadrupole matrix elements a value of $-.8$ barn is used.

Similarly, in Figure 9, we display the projectile excitation effects as functions of the bombarding energy. A value of $-.07$ barn is used for the reduced $E2$-matrix elements $\langle 5/2 \| \mathcal{M}(E2) \| 1/2 \rangle$, $\langle 5/2 \| \mathcal{M}(E2) \| 5/2 \rangle$ of ^{17}O.

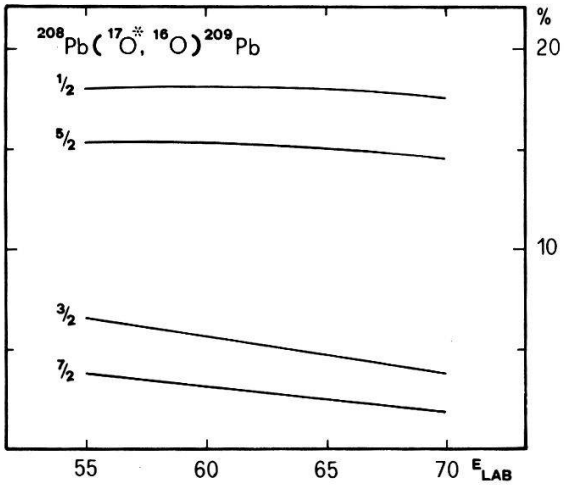

Figure 9
The energy dependence of the projectile excitation effects in four levels of ^{209}Pb. A value of $-.07$ barn is used for the $E2$-couplings $M^P_{5/2\,5/2}$ and $M^P_{5/2\,1/2}$ of ^{17}O.

4.6. *Dependence of the EEF on the projectile*

The number of different indirect transitions which contribute to the excitation effects naturally depends very much on the projectile. It is immediately clear that the effects of projectile excitation will depend upon the number of low-lying levels. The rules established in the theory of Coulomb excitation [10] can be applied to answer the question if projectile excitation will play an important role. Furthermore, in most cases, the electric quadrupole matrix elements between the low-lying projectile states have been experimentally measured, so that the effects of projectile excitation on the neutron transfer cross-section can be computed.

On the other hand, the target levels, via which the contributive indirect transitions take place, are roughly all neighbouring levels populated to a similar or higher degree than the state in question.

Finally, the target excitation effects depend upon the projectile charge Z_1. If only reactions at the Coulomb barrier are composed, the target excitation effects are approximately proportional to Z_1. For deuteron stripping reactions, they can in general be neglected.

In Figures 10 and 11, the EEF $E^T_{z5/2}(\vartheta)$ which describe the target excitation effect in the $5/2^+$ state, are displayed for the reactions ^{208}Pb(^{17}O, ^{16}O)^{209}Pb and ^{208}Pb(^{13}C, ^{12}C)^{209}Pb. While for the ^{17}O projectile four intermediate target states contribute significantly, in the case of the ^{13}C projectile only two indirect transitions give considerable excitation effects. This is due to the fact that for the ^{13}C projectile the transfer transitions into the $7/2^+$ and $3/2^+$ state occur with far lower probability than those into the $5/2^+$ and $1/2^+$ state. This can be explained by the following rule:

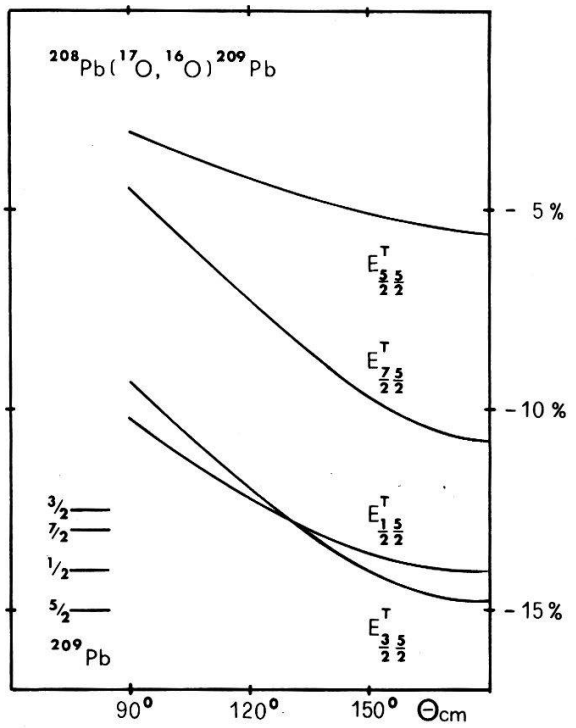

Figure 10
For the reaction ^{208}Pb(^{17}O, ^{16}O)^{209}Pb at a laboratory energy of 70 MeV the effect functions $E^T_{zf}(\vartheta)$ are plotted for the final state $5/2^+$ at 1.56 MeV in ^{209}Pb. Apart from the reorientation in the $5/2^+$ state, three higher-lying levels contribute to the excitation effect.

Transitions from an initial state with $j = l - \frac{1}{2}$ will favourably take place into final states with $j' = l' + \frac{1}{2}$ [5, 8].

This rule is a consequence of the selection rules (2) and of the fact that the highest possible angular momentum transfer gives the largest contribution to the transition amplitudes.

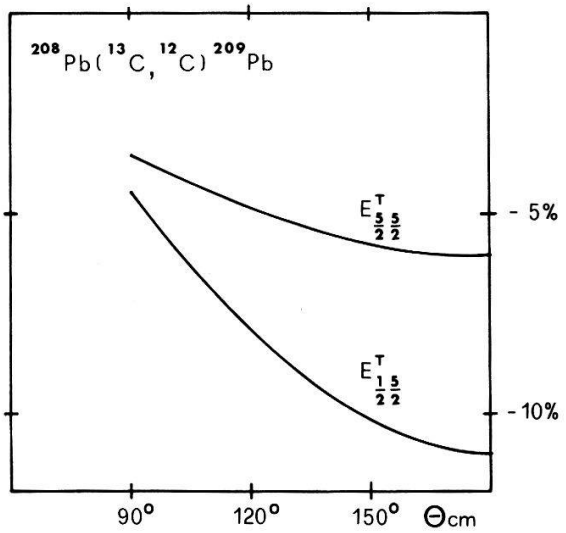

Figure 11
For the reaction ^{208}Pb(^{13}C, ^{12}C)^{209}Pb at a laboratory energy of 45 MeV the effect functions $E^T_{zf}(\vartheta)$ are shown for the final state $5/2^+$ in ^{209}Pb. Apart from the reorientation effect in the $5/2^+$ state, only one higher-lying state, the $1/2^+$ state at 2.01 MeV, contributes to the excitation effect.

4.7. *Realistic examples for the virtual excitation effects in NTR*

In order to estimate the Coulomb excitation effects that will occur in realistic neutron transfer reactions, we have used single particle values for the electric quadrupole matrix elements [12] for the computation of the excitation effects in the reactions ^{208}Pb(^{17}O, ^{16}O)^{209}Pb at 70 MeV and ^{206}Pb(^{21}Ne, ^{20}Ne)^{207} at 85 MeV.

In Figures 12 and 13, we show the EEF for these two reactions as functions of the centre of mass scattering angle Θ_{cm}.

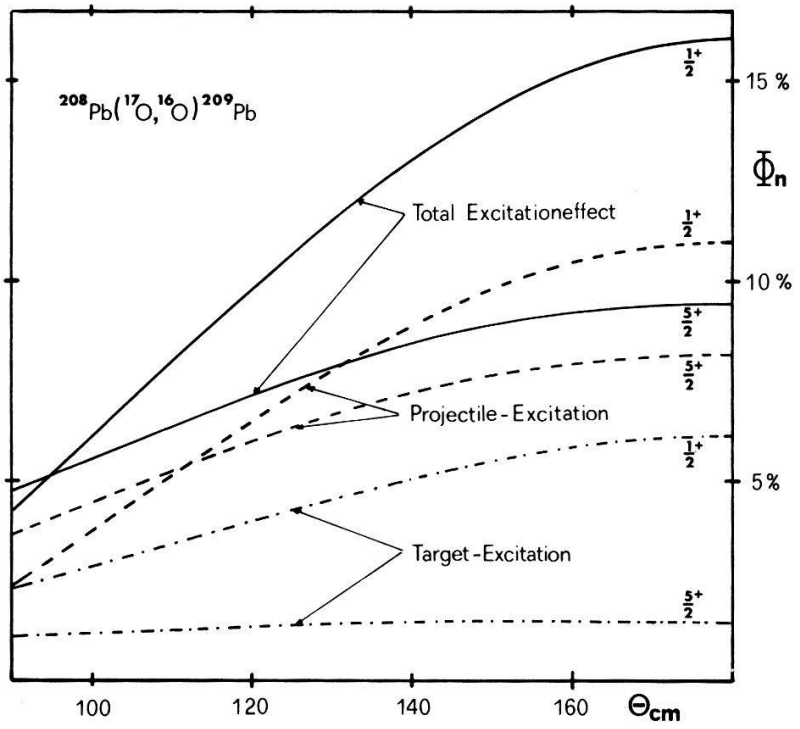

Figure 12
For the reaction ^{208}Pb(^{17}O, ^{16}O)^{209}Pb at 70 MeV laboratory energy the Coulomb excitation effect in four levels of ^{209}Pb is shown. For the reduced $E2$-matrix elements in ^{209}Pb the single particle values, as given by True and Ford, have been used. Experimental values for the reduced $E2$-matrix elements of ^{17}O have been employed.

4.8. *The determination of electric quadrupole matrix elements from measured differential transfer cross-sections*

In order to obtain experimental values for the excitation effect functions from measurements of the differential neutron transfer cross-section $(d\sigma_f/d\Omega)^{exp}$ it is appropriate to form the experimental ratio

$$R_f^{exp}(\vartheta) = \left(\frac{d\sigma_f(\vartheta)}{d\Omega}\right)^{exp} \Bigg/ \left(\frac{d\sigma_f(\vartheta_N)}{d\Omega}\right)^{exp} \tag{87}$$

and the theoretical ratio

$$R_f^{th}(\vartheta) = \left(\frac{d\sigma_f(\vartheta)}{d\Omega}\right)^{th} \Bigg/ \left(\frac{d\sigma_f(\vartheta_N)}{d\Omega}\right)^{th} \tag{88}$$

which is a function of the reduced quadrupole matrix elements. The normalization angle ϑ_N is chosen such as to assure that the influence of the nuclear interaction on the experimental ratio $R_f^{\exp}(\vartheta)$ can be neglected. If the reaction proceeds at bombarding energies well below the Coulomb barrier, a value of 180 degrees can be used for ϑ_N.

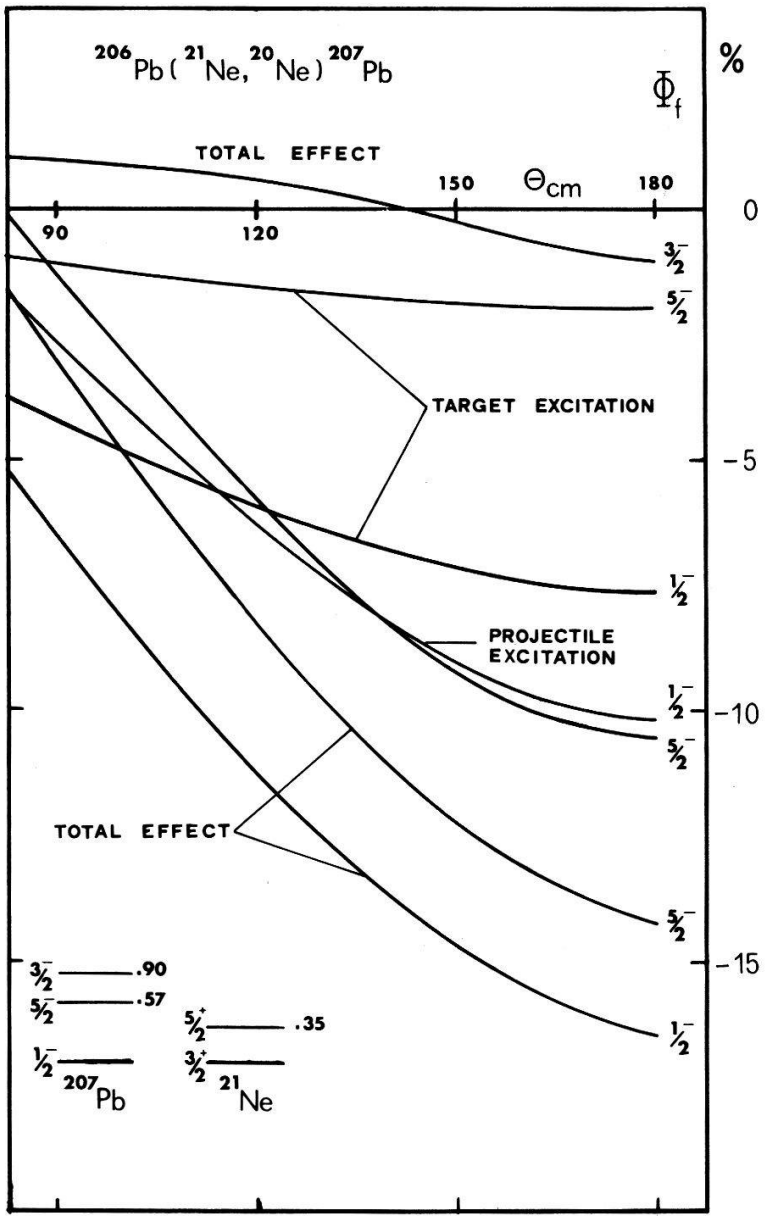

Figure 13
For the reaction ^{206}Pb(^{21}Ne, ^{20}Ne)^{207}Pb at 85 MeV laboratory energy the Coulomb excitation effects in the first three levels of 207Pb are shown. For the reduced $E2$-matrix elements in ^{207}Pb the single particle values [12] have been used, while for those of ^{21}Ne experimental values have been employed.

The theoretical ratio $R_f^{\text{th}}(\vartheta, M_{rs})$ can be written in terms of the excitation effect functions, as following

$$R_f^{\text{th}}(\vartheta, M_{rs}) = R_f^{\text{th}}(\vartheta, M_{rs}=0)\frac{1+\phi_f(\vartheta, M_{rs})}{1+\phi_f(\vartheta_N, M_{rs})}, \tag{89}$$

where the theoretical value of the ratio function $R_f^{\text{th}}(\vartheta, M_{rs}=0)$ for vanishing M_{rs} has been extracted. The condition for fitting the theoretical values of the neutron transfer

cross-sections to the measured ones, described by

$$R_f^{\text{th}}(\vartheta, M_{rs}) = R_f^{\text{exp}}(\vartheta) \tag{90}$$

can be written in the form

$$\frac{R_f^{\text{exp}}(\vartheta)}{R_f^{\text{th}}(\vartheta, M_{rs}=0)} = \frac{1+\phi_f(\vartheta, M_{rs})}{1+\phi_f(\vartheta_N, M_{rs})}. \tag{91}$$

We know that the excitation effect functions practically only depend upon the reduced quadrupole matrix elements and ratios of spectroscopic factors. To a good approximation, these ratios can be determined from the relative magnitudes of the cross-sections for transfer to neighbouring levels. We may thus hope that under favourable experimental conditions a determination of quadrupole matrix elements from the measured angular distributions of neutron transfer cross-sections is feasible.

Acknowledgments

We would like to thank Dres. G. Baur, F. Rösel, D. Trautmann and dipl. phys. M. Pauli for many helpful discussions.

REFERENCES

[1] P. J. A. Buttle and L. J. B. Goldfarb, Nucl. Phys. *78*, 409 (1966).
[2] G. Breit and M. Ebel, Phys. Rev. *104*, 1030 (1956).
[3] K. Alder and A. Winther, Kgl. Danske Videnskab. Selskab. Mat. Fys. Medd. *32* (No. 8) (1960).
[4] P. J. A. Buttle and L. J. B. Goldfarb, Nucl. Phys. *A176*, 299 (1971).
[5] K. Alder, R. Morf, M. Pauli and D. Trautmann, Nucl. Phys. *A191*, 399 (1972).
[6] D. Trautmann and K. Alder Helv. Phys. Acta *43*, 363 (1971).
[7] K. Alder and D. Trautmann, Nucl. Phys. *A178*, 60 (1971).
[8] R. A. Broglia and A. Winther, Nucl. Phys. *A182*, 112 (1972).
[9] H. Ritter, Diplomarbeit, unpublished.
[10] K. Alder, A. Bohr, T. Huus, B. Mottelson and A. Winther, Rev. Mod. Phys. *28*, 432 (1956).
[11] M. Pauli, Diplomarbeit, unpublished.
[12] W. W. True and K. W. Ford, Phys. Rev. *109*, 1675 (1958).
[13] A. Winther and J. de Boer, Cal. Tech. technical report, Nov. 18, 1965, reprinted in K. Alder and A. Winther, *Coulomb Excitation* (Academic Press, New York 1966).